Bulletin of the Seismological Society of America, Vol. 96, No. 4B, pp. S1–S10, September 2006, doi: 10.1785/0120050831

Introduction to the Special Issue on the 2004 Parkfield Earthquake and the Parkfield Earthquake Prediction Experiment

by Ruth A. Harris and J Ramón Arrowsmith

Abstract The 28 September 2004 **M** 6.0 Parkfield earthquake, a long-anticipated event on the San Andreas fault, is the world's best recorded earthquake to date, with state-of-the-art data obtained from geologic, geodetic, seismic, magnetic, and electrical field networks. This has allowed the preearthquake and postearthquake states of the San Andreas fault in this region to be analyzed in detail. Analyses of these data provide views into the San Andreas fault that show a complex geologic history, fault geometry, rheology, and response of the nearby region to the earthquake-induced ground movement. Although aspects of San Andreas fault zone behavior in the Parkfield region can be modeled simply over geological time frames, the Parkfield Earthquake Prediction Experiment and the 2004 Parkfield earthquake indicate that predicting the fine details of future earthquakes is still a challenge. Instead of a deterministic approach, forecasting future damaging behavior, such as that caused by strong ground motions, will likely continue to require probabilistic methods. However, the Parkfield Earthquake Prediction Experiment and the 2004 Parkfield earthquake have provided ample data to understand most of what did occur in 2004, culminating in significant scientific advances.

Introduction

On 28 September 2004 a moment magnitude (**M**) 6.0 earthquake struck the Parkfield region of the San Andreas fault in central California (Bakun *et al.*, 2005; Langbein *et al.*, 2005) (Fig. 1). Due to its occurrence in a sparsely populated region of California, the earthquake caused no injuries to the inhabitants of the area (San Luis Obispo County Office of Emergency Services, 28 September 2004), but it did still destroy some nonstructural parts of buildings, in addition to building contents (e.g., Goel and Chadwell, 2004). This long-anticipated earthquake was monitored by a wealth of scientific instrumentation designed to record it, most of which was part of the Parkfield Earthquake Prediction Experiment (Bakun and Lindh, 1985; Roeloffs and Langbein, 1994; Roeloffs, 2000). The San Andreas fault's best-known and well-studied section is that which ruptured in 2004. The results from studies representing a range of geophysical and geological subdisciplines have provided an essential characterization of the San Andreas fault zone, faulting and rock mechanics, and earthquake occurrence in general. Observation and analysis of the 2004 event are highlights of this scientific experiment. As a result, researchers are now able to answer a number of questions about the nature of earthquake behavior. Those answers include the following:

1. Predicting the general timing and size of moderate and large earthquakes is difficult. At Parkfield, although the timing of **M** 6.0 events may not be random (Bakun *et al.*, 2005), simple ideas of earthquake recurrence such as the characteristic, time-predictable, and slip-predictable models did not work for the 2004 mainshock (Jackson and Kagan, 2006; Murray and Langbein, 2006). Jackson and Kagan (2006) also suggest that preselection of magnitude for the Parkfield earthquakes is what led to the apparently nonrandom recurrence statistics.
2. Magnitude 6.0 earthquakes can occur without detectable short-term precursors (Borcherdt *et al.*, 2006; Johnston *et al.*, 2006a,b; Langbein *et al.*, 2005).
3. Ground-motion variability is substantial in the near field, and source, path, and site effects all play important roles in the variability (Borcherdt *et al.*, 2006; Fletcher *et al.*, 2006; Liu *et al.*, 2006; Shakal *et al.*, 2005, 2006a,b).
4. High ground motions, liquefaction, and slumping may result from a shallow earthquake even though there is minimal surface slip (Rymer *et al.*, 2006).
5. Earthquake rupture extent may be affected by fault rheology (Michael and Eberhart-Phillips, 1991; Lees and Nicholson, 1993; Waldhauser *et al.*, 2004; Langbein *et al.*, 2005; Murray and Segall, 2005; Fletcher *et al.*, 2006; Murray and Langbein, 2006; Thurber *et al.*, 2006), but earthquake rupture direction may not be predictable on the basis of classic observables, such as ma-

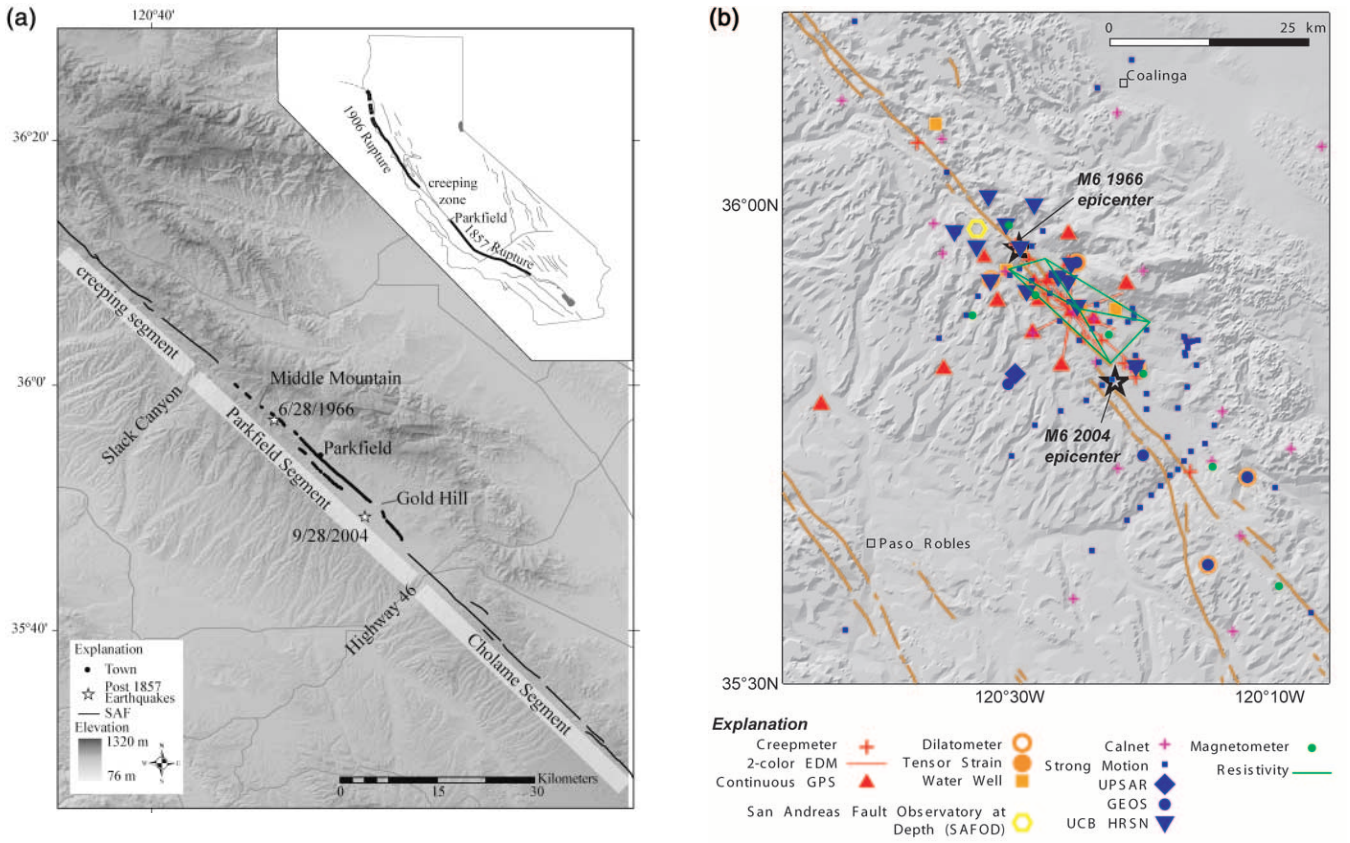

Figure 1. Setting of the 2004 **M** 6.0 Parkfield, California, earthquake and the Parkfield Earthquake Prediction Experiment. (a) Map view of Parkfield's location between contrasting zones of fault behavior along the San Andreas fault (SAF) in California. To the northwest of Parkfield the SAF slips in creep and small earthquakes and to the southeast the SAF last slipped in the 1857 **M** 7.9 Fort Tejon earthquake. The grayscale hill shading over a 90-m Digital Elevation Map (DEM) is overlain by historic surface traces of the SAF (Jennings, 1977) (thin black line), the 2004 Parkfield rupture trace (Rymer *et al.*, 2006) (thick black line), the 1966 and 2004 mainshock epicenters, and important geographic features (modified from Toké and Arrowsmith, 2006). (b) Scientific instrumentation deployed in the Parkfield region during the Parkfield Earthquake Prediction Experiment. UPSAR, USGS Parkfield Dense Seismograph Array (Fletcher *et al.*, 2006); GEOS, General Earthquake Observation System (Borcherdt *et al.*, 2006), 2-color EDM, two-color Electronic Distance Meter, a laser geodetic network (Langbein *et al.*, 2006). UCB HRSN, University of California, Berkeley High Resolution Seismic Network. SAFOD, deep borehole observatory (see http://earthscope.org/safod and Hickman *et al.* [2004]). Figure courtesy of Parkfield Chief Scientist, John Langbein.

terial contrasts near faults (Harris and Day, 1997, 2005, 2006; Andrews and Harris, 2005, 2006; Xia *et al.*, 2005).

6. Even with numerous types of observations (e.g., surface-slip measurements, Interferometric Synthetic Aperture Radar [InSAR], Global Positioning System [GPS]; strong ground motion), it may be difficult to reconcile a single highly detailed deep-slip model for an earthquake. However a picture can emerge that shows distinct slip features consistent with all of the observations (Custodio *et al.*, 2005; Johanson *et al.*, 2006; Johnston *et al.*, 2006a; Langbein *et al.*, 2006; Liu *et al.*, 2006; Murray and Langbein, 2006).
7. The locations of subsequent smaller earthquakes (aftershocks) may not be predictable on the sole basis of stress changes due to the mainshock. For Parkfield, fault rheology also appears to play a key role in determining where small aftershocks and continuous microseismicity occur (Waldhauser *et al.*, 2004, Bakun *et al.*, 2005; Fletcher *et al.*, 2006; Johanson *et al.*, 2006; Langbein *et al.*, 2006; Murray and Langbein, 2006; Thurber *et al.*, 2006). Alternatively, a broad picture of the size distributions of continuous microseismicity may help illuminate the region that eventually ruptures in a mainshock (Schorlemmer and Wiemer, 2005).
8. The San Andreas fault appears to be segmented in the Parkfield area such that the 2004 and prior events were contained in the expected fault region (e.g., Bakun and

Lindh, 1985; Michael and Jones, 1998). The segmentation may be partly defined by surficial fault geometry and slip behavior. However, the accumulation and release of strain has a gradient in the middle of the Parkfield segment with little slip deficit over the last several earthquake cycles from near the town of Parkfield to the northwest. This is largely due to higher interseismic creep rates to the northwest (e.g., Murray and Langbein, 2006; Toké and Arrowsmith, 2006). While more paleoseismic data are needed for the Parkfield area, the studies of Toké *et al.* (2006) can be interpreted with repeating moderate earthquakes and creep in the Parkfield area and do not require large (multimeter) surface rupture.

9. The moment release of some mainshocks exceeds that released postseismically. Interestingly, this is not the case for the 2004 Parkfield earthquake where postseismic moment release (after about 100 sec of the mainshock) is similar to that released coseismically (Langbein *et al.*, 2006; Lienkaemper *et al.*, 2006; Johanson *et al.*, 2006; Murray and Langbein, 2006). In addition, during the 2004 Parkfield earthquake, the coseismic and postseismic slip migrated spatially as a function of time (Johanson *et al.*, 2006; Johnson *et al.*, 2006; Langbein *et al.*, 2006; Murray and Langbein, 2006).
10. Despite the complex details of Parkfield earthquakes and the San Andreas fault zone, the long-term (million year) evolution of the San Andreas near Parkfield can be understood by modeling the basic interaction between the creeping and locked portions of the fault (Simpson *et al.*, 2006). Evidence for this resides in the fault geometry and fault geology, with the Parkfield section of the San Andreas fault showing slip variations along adjacent fault strands (Southwest Fracture Zone and main San Andreas fault) over timescales varying from the 2004 event (Langbein, *et al.*, 2006; Simpson *et al.*, 2006) to the million year timescale (e.g., Sims, 1990; Rymer *et al.*, 2003; Thayer *et al.*, 2004; Thayer, 2006).

The Parkfield experiment was designed in the mid-1980s, at a time when it appeared that similar **M** 6.0 earthquakes occurred fairly regularly near Parkfield (Bakun and McEvilly, 1984; Bakun and Lindh, 1985). The Parkfield sequence has included **M** 6.0 earthquakes in 1881, 1901, 1922, 1934, 1966, and 2004 (see Bakun *et al.* [2005] for information about the magnitudes of the older earthquakes). The 1966 earthquake was carefully examined by field geologists (e.g., Brown *et al.*, 1967) and recorded by strong ground motion and geodetic instruments, and similar to the 2004 event, led to a considerable number of scientific advances (for starters, see the *Bulletin of the Seismological Society of America* Special Issue on the 1966 earthquake, vol. 57, no. 6, 1967) including basic ideas about earthquake source behavior and the resulting short-term strong ground motions and longer-term postseismic fault behavior.

Many of the expectations for the next Parkfield earthquake following 1966 were based on the known characteristics of its **M** 6.0 predecessors (Michael and Jones, 1998), such as the epicenter, magnitude, rupture direction, rupture extent, and surface cracking (Bakun and McEvilly, 1984). Although the 2004 event did not fulfill all of these expectations, it was due to this optimism of a potentially predictable earthquake that so many instruments were installed and maintained in place to capture the 2004 event.

In this article we discuss some of the new advances brought to light by the 2004 earthquake and the Parkfield Earthquake Prediction Experiment. We also encourage the reader to consult comprehensive overviews of the Parkfield Earthquake Prediction Experiment by Roeloffs and Langbein (1994) and Roeloffs (2000), and preliminary reviews of data generated by the 2004 Parkfield earthquake by Bakun *et al.* (2005), Bilham (2005), Langbein *et al.* (2005), and Shakal *et al.* (2005). In Table 1 we list the articles included in the special issue and the general subject areas that they cover.

Results and Discussion

Energy Budgets and Time-Predictable versus Slip-Predictable Earthquakes

Most mechanical models of faulting and earthquakes assume that there is an energy budget and that the energy accumulation and release rates along shallow portions of faults need to keep up with the deeper portions of faults over some period of time. The differences in the predictions of earthquake recurrence, then, depend on the time over which this energy balance needs to occur and the mechanics of fault loading and failure. One simple prediction approach for earthquake recurrence is the concept of the time-predictable earthquake (Bufe, 1977; Shimazaki and Nakata, 1980). The time-predictable model assumes that fault failure (an earthquake) occurs when a fixed fault yield strength is reached. Therefore the time to the next earthquake is set by the amount of slip in the last earthquake. In the time-predictable model, the next earthquake should occur as soon as the amount of slip in the last earthquake has accumulated as a slip deficit whereby the shallower portions of the fault are that much behind the deeper, constantly slipping portions of the fault. Assuming the time-predictable model at Parkfield, the time to the earthquake following 1966 was set by the amount of slip that occurred in the 1966 earthquake. Harris and Segall (1987), Murray *et al.* (2001), Murray and Segall (2002), and Segall and Harris (1986, 1987) did this calculation and all showed that the slip deficit in the shallow portions of the fault at Parkfield was reaccumulated long before 2004. Therefore the time-predictable model has not worked at Parkfield (Murray and Langbein, 2006).

Earthquake interaction effects have been explored as an explanation for the time delay of the Parkfield earthquake. Stress change effects due to the nearby 1983 **M** 6.4 Coalinga

Table 1
Special Issue Articles and General Subject Areas

Authors	Theme(s)
Rymer *et al.*	Geologic data
Simpson *et al.*	Tectonics, seismicity, fault-geometry models
Thurber *et al.*	Seismicity data, velocity structure models
Dost and Haak	Seismic data, teleseismic waveform data
Johnston *et al.* (a)	Strain data, precursors, prediction, nucleation models
Borcherdt *et al.*	Strong ground motion data, fault-slip models, precursors
Shakal *et al.* (a)	Strong ground motion data
Shakal *et al.* (b)	Strong ground motion data
Fletcher *et al.*	Strong ground motion data, fault-slip models
Liu *et al.*	Strong ground motion fault-slip models
Wang *et al.*	Strong ground motion parameters
Mena *et al.*	Strong ground motion modeling methods
Johnston *et al.* (b)	Seismomagnetic data, prediction
Toké *et al.*	Paleoseismic data and models
Lienkaemper *et al.*	Geodetic data, geologic data
Titus *et al.*	Geodetic data
Johanson *et al.*	Geodetic data, fault-slip models, fault mechanics
Murray and Langbein	Geodetic data, fault-slip models, prediction
Langbein *et al.*	Geodetic data, fault-slip models, fault mechanics
Johnson *et al.*	Geodetic fault-slip models, fault mechanics
Toké and Arrowsmith	Geologic slip data, strain budget models
Li *et al.*	Seismic data, cracks, damage, fault-zone structure models
Cochran *et al.*	Seismic data, cracks, damage models
Shcherbakov *et al.*	Aftershock statistics models
Toppozada and Branum	Historical earthquake data and forecasting
Jackson and Kagan	Prediction

earthquake have been credited with delaying the Parkfield earthquake by up to a few years (Simpson *et al.*, 1988; Toda and Stein, 2002). However, even with this delay, the occurrence of the most recent **M** 6.0 earthquake in 2004 is still inconsistent with the time-predictable model. It has also been proposed that interaction effects due to the distant **M** 7.9 1906 and nearby **M** 7.9 1857 earthquakes have modulated the timing of **M** 6.0 Parkfield earthquakes (Ben-Zion *et al.*, 1993). While intriguing, this idea may need more features to explain why the times between successive Parkfield **M** 6.0 have not been progressively longer (i.e., this idea works well for the successively longer 1934–1966 and 1966–2004 time intervals, but does not explain why a short interval suddenly appeared from 1922 to 1934, following longer intervals from 1881 to 1901 and 1901 to 1922). Alternatively, this idea of lengthening interevent times may be consistent if additional earthquakes in the surrounding region are considered (Toppozada and Branum, 2006).

Similar to the time-predictable model, the slip-predictable earthquake model also appears unsatisfactory at Parkfield (Bakun and McEvilly, 1984; Jackson and Kagan, 2006; Lienkaemper *et al.*, 2006; Murray and Langbein, 2006; Toké and Arrowsmith, 2006). In the slip-predictable model a fixed lower level of fault strength sets the slip in the next earthquake to be determined by the amount of time that has elapsed since the last earthquake. According to the slip-predictable model, much more slip should have occurred in the 2004 Parkfield earthquake, leading to a larger magnitude event than the actual **M** 6.0 (e.g., Harris and Archuleta, 1988; Arrowsmith *et al.*, 1997; Murray and Langbein *et al.*, 2006).

Given that the San Andreas fault zone in the Parkfield region also releases some of its energy aseismically (fault slip without generation of seismic waves) in addition to seismically (fault slip with generation of seismic waves), some investigators have calculated the energy budget by including the aseismic slip that occurs right after Parkfield earthquakes. The addition of the aseismic slip does make a significant difference in the magnitude of the total slip events at Parkfield (Murray and Segall, 2005; Johanson *et al.*, 2006; Johnson *et al.*, 2006; Langbein *et al.*, 2006; Murray and Langbein, 2006; Toké and Arrowsmith, 2006), but still does not satisfy the slip-predictable model. This earthquake is the first time that slip as a function of time has been imaged in detail, due to the extensive Parkfield Earthquake Prediction Experiment networks of strong ground motion stations, creep meters, alignment arrays, and GPS stations at frequencies starting at 1 Hz. However, even with this detailed imaging, it is still clear that the substantial postseismic slip following **M** 6.0 Parkfield earthquakes does not catch the shallower parts of the fault up to the longer-term slip rates of the deeper parts of the San Andreas fault. Instead, the largest earthquakes on the fault, such as the **M** 7.9 1857 Ft. Tejon event, likely dominate in the energy equation (Toké and Arrowsmith, 2006).

Time-predictable or slip-predictable models are some-

times featured elements in earthquake hazard assessments (e.g., Jackson and Kagan, 2006). Because **M** 6.0 earthquakes at Parkfield fit neither time nor slip-predictable models of earthquake recurrence, the question is if these recurrence concepts should be applied elsewhere. One could argue that **M** 6.0 earthquakes are not the largest events that occur in the Parkfield region, instead **M** 7.9–**M** 8 events dominate the strain budget, so perhaps these largest events are what should be tested instead. A challenge is that the most recent **M** 7.9 earthquake thought to have started at Parkfield is not clearly revealed in the paleoseismic trenches at Parkfield (Toké *et al.*, 2006), but major slip is apparent southeast of Parkfield along the fault (Grant and Sieh, 1993, 1994; Young *et al.*, 2002).

The gradient in interseismic slip and slip deficit along the Parkfield segment (e.g., Murray *et al.*, 2006; Toké and Arrowsmith, 2006) may suggest that while the segmentation concept works in that the Parkfield segment contained the 2004 event, it does not work so well in that the 1857 event may have ruptured into the southern portion of the segment (slip measurements of Sieh, [1978a,b] and Lienkaemper [2001]). However, the exposures of Toké *et al.* (2006) can be interpreted by repeating moderate earthquakes and creep in the Parkfield area and do not require large (multimeter) surface rupture, so perhaps 1857 terminated somewhere between Highway 46 and the town of Parkfield (e.g., Lienkaemper *et al.*, 2006; Toké and Arrowsmith, 2006).

Paleoseismic investigations even farther southeast on the San Andreas fault, at Wrightwood, reveal irregular earthquake recurrence, and it has been posited that these events also do not fit the simple times or slip-predictable models (Weldon *et al.*, 2004). Because these investigations are point measurements and the amount of slip per event is often unknown, future study is needed to help resolve the issue. In the case of Parkfield, this includes more coverage along the main San Andreas fault as well as information on the paleoseismic behavior of the Southwest Fracture Zone.

Precursors

The utility of short-term earthquake prediction has been proposed by some yet dismissed by others in the scientific community. This type of prediction might involve precursory signals that could alert scientists and the public seconds to days in advance of a pending earthquake hazard. With this goal in mind, numerous sensors were deployed at Parkfield to record potential precursory signals. The instruments included water wells, high-resolution strain, electric field, magnetic field, and seismic-wave detectors. It appears that nothing unusual (statistically significant) was recorded before the 2004 Parkfield mainshock (Bakun *et al.*, 2005; Borcherdt *et al.*, 2006; Johnston *et al.*, 2006a,b). Unlike the previous two Parkfield **M** 6.0 earthquakes in 1934 and 1966, but similar to the **M** 6.0 Parkfield earthquakes in 1901 and 1922, there were no **M** 5 foreshocks in 2004, and no other notable precursory signals were recorded on any of the sensors.

Even without precursory signals, measurements before, during, and after a mainshock provide constraints on nucleation and subsequent earthquake processes. For example, the Parkfield data provide good comparisons among the various types of coseismic and postseismic signals caused by the **M** 6.0 earthquake (Johnston *et al.* 2006b). The Parkfield data also provide constraints on the nucleation process during the mainshock. Johnston *et al.* (2006a) find that the nucleation zone was probably smaller than 30 m in size and released less moment than a **M** 2.2 earthquake.

Ground Motions

The **M** 6.0 Parkfield earthquake produced highly variable patterns of ground motions in the near-field region (Shakal *et al.*, 2005, 2006a; Borcherdt *et al.*, 2006; Fletcher *et al.*, 2006; Wang *et al.*, 2006). The highest recorded ground motions were greater than 2*g* acceleration and 80 cm/sec velocity in the fault-normal direction on a soil site station, Fault Zone 16 (Shakal *et al.*, 2006b). This peak acceleration is among the highest ever recorded.

Bakun *et al.* (2005), Shakal *et al.* (2006a), and Wang *et al.* (2006) compare the Parkfield ground-motion recordings with some of the ground-motion attenuation relations currently in use. The attenuation relations are measures of how ground motions change with distance from a fault. The attenuation relations appear consistent with the Parkfield data, in terms of both the median values and the variability, but the high ground motion at FZ16 (Shakal *et al.*, 2006b) demonstrate why one should not be truncating the ground-motion distribution at one or two sigma in the attenuation relations (Norm Abrahamson, personal comm., 2006). Additionally, the wide range of ground motion recorded at Parkfield in the near-field (Fletcher *et al.*, 2006 Shakal *et al.*, 2006a,b; Wang *et al.*, 2006) emphasize why it is necessary to use a probabilistic approach for design ground motions (Norm Abrahamson, personal comm., 2006).

Source, path, and site effects all played important roles in determining the ground motions produced by the 2004 Parkfield earthquake. Stations that were in place during 2004, as well as during earlier events, such as the 1983 **M** 6.4 Coalinga earthquake and 2003 **M** 6.5 San Simeon earthquake (Hardebeck *et al.*, 2004), were often, but not always, affected differently by each earthquake. Liu *et al.* (2006), Shakal *et al.* (2006a,b), and Wang *et al.* (2006) discuss these interearthquake comparisons. Fletcher *et al.* (2006) and Wang *et al.* (2006) note the marked near-field variability among the close stations in the U.S. Geological Survey Parkfield Dense Seismograph Array (UPSAR) that recorded the 2004 mainshock and show how detailed features of the path (i.e., velocity structure of the fault region and the ground surface topography) in addition to the source, affected the ground motions. Clearly probabilistic approaches will be necessary to forecast the ground-motion variability caused

by all future large earthquakes (Norm Abrahamson, personal comm., 2006).

Source Behavior

The coseismic slip during the 2004 mainshock was observed geologically at the Earth's surface (Lienkaemper *et al.*, 2006, Rymer *et al.*, 2006) and inferred at depth using surface slip, creep, alignment array, GPS, InSAR, strong ground motion, strain, and magnetic data (Borcherdt *et al.*, 2006; Custodio *et al.*, 2005; Fletcher *et al.*, 2006; Johanson *et al.*, 2006; Langbein *et al.*, 2006; Lienkaemper *et al.*, 2006; Liu *et al.*, 2006; Murray and Langbein, 2006; Mena *et al.*, 2006). Constraints on the geodetic models for deep slip were assisted by estimates of slip rates for the creeping section to the north (Titus *et al.*, 2006). It should be noted that the Parkfield earthquake is probably the first time that such a comprehensive geodetic data set has been recorded for a mainshock and its immediate postseismic period. These data sets, along with the newly revealed geometry (Simpson *et al.*, 2006 Thurber *et al.*, 2006) and velocity structure of the fault of the San Andreas fault zone in this region (Cochran *et al.*, 2006; Li *et al.*, 2006; Thurber *et al.*, 2006) have allowed for an unprecedented view of an **M** 6.0 earthquake, and the mechanical transition of a fault and its surroundings into the postseismic period.

Inclusion of detailed fault zone geometry allowed Murray and Langbein (2006) to show temporal migration of slip from one fault strand to another. Availability of high-rate GPS and strain data allowed for investigations of the transition from coseismic to postseismic response of the fault zone (Johnson *et al.*, 2006; Langbein *et al.*, 2006). Unlike some earthquakes where postseismic slip may be a small fraction of the mainshock, at Parkfield the postseismic slip was revealed to be comparable to that of the mainshock (e.g., Johanson *et al.*, 2006; Johnson *et al.*, 2006; Langbein *et al.*, 2006; Murray and Langbein, 2006). Similar behavior was suspected for previous **M** 6.0 Parkfield earthquakes, and sizeable afterslip was observed at the earth's surface following the 1966 event (e.g., Allen and Smith, 1966), but before 2004 the geodetic data did not allow separation of the (deep) mainshock slip from comingled mainshock and postseismic slip, due to less frequent (and more difficult to collect) geodetic measurements in earlier decades.

Using the high-rate GPS and strain data from the 2004 Parkfield earthquake, Langbein *et al.* (2006) and Johnson *et al.* (2006) analyzed the transition from coseismic to postseismic periods. Langbein *et al.* (2006) determined that the observed behavior from 100 sec to 9 months following the 2004 mainshock is consistent with creep models for elastic solids. Johnson *et al.* (2006) looked at possible afterslip, poroelastic, and viscoelastic effects. They determined that rate-state friction and a simple model of afterslip on the fault plane fits the postseismic data in the first few months following the 2004 earthquake.

Comparisons of the strong-motion-derived models for the 2004 mainshock and the geodetically inferred models show some similarities and some differences. It should be noted though that the two data sets have different resolving capabilities that partly depend on each network's spatial coverage on the Earth's surface. Overall, a comparison of the geodetic and seismological models image the major coseismic slip occurring northwest of the Gold Hill hypocenter (Custodio *et al.*, 2005; Johanson *et al.*, 2006; Johnson *et al.*, 2006; Liu *et al.*, 2006; Murray and Langbein, 2006). Discrepancies include whether or not major slip also occurred at the hypocenter, with the strong ground motion inversion and forward modeling (Custodio *et al.*, 2005; Liu *et al.*, 2006; Shakal *et al.*, 2006a) inferring considerable slip at the hypocenter, and the high-rate of sampling geodetic inversions not imaging slip at the hypocenter (Johnson *et al.*, 2006; Langbein *et al.*, 2006; Murray and Langbein, 2006). Interestingly, the study by Johanson *et al.* (2006) that included lower frequency GPS, in addition to InSAR data, did image slip at the hypocenter. It is quite possible that these differences may be reconciled with a look at the temporal and spatial station resolution, as demonstrated in models by Langbein *et al.* (2006), and Johnson *et al.* (2006) that force slip to occur at the hypocenter and still satisfactorily fit the geodetic data. This question may be solved with joint strong-motion/geodetic-data inversions that carefully consider the resolving capabilities of each data set. Future work may also consider a more accurate fault geometry model in the ground-motion inversions, as was done for the geodetic inversions by Murray and Langbein (2006).

Rupture extent was one part of the successful definition of Parkfield earthquakes outlined by Michael and Jones (1998) for the Parkfield source, with the expectation that the $\mathbf{M} \geq 5.7$ earthquake(s) following 1966 would repeat certain aspects of the 1966 mainshock and its **M** 6.0 predecessors. Fortunately for the Michael and Jones (1998) definition, they, unlike Bakun and McEvilly (1984) and Bakun and Lindh (1985) did not assume a rupture propagation direction to the southeast. The 2004 earthquake, although it appeared similar to its predecessors in 1922, 1934, and 1966 at teleseismic distances (Dost and Haak, 2006), appears to have primarily ruptured to the northwest, with perhaps a bilateral component of short southeast rupture (Custodio *et al.*, 2005; Liu *et al.*, 2006; Shakal *et al.*, 2006a). There has been some debate (with one viewpoint represented by Ben-Zion [2006] and the other viewpoint represented by Harris and Day [2005, 2006] and Xia *et al.* [2005]) about whether or not the 2004 earthquake should have propagated either to the northwest or bilaterally, considering the material contrast across the fault zone revealed by Eberhart-Phillips and Michael (1993) and Thurber *et al.* (2006). However, theoretical studies by Harris and Day (1997, 2005) and Andrews and Harris (2005) of the behavior of an earthquake rupture near a material contrast show the 2004 Parkfield earthquake to be fully consistent with our physics-based understandings of earthquake behavior. Earthquake ruptures depend on not just the material properties of the surrounding rocks, but also depend

on the fault geometry, fault friction, and perhaps most importantly, the state of stress on the fault (Harris, 2004; Andrews and Harris, 2005).

Li *et al.* (2006) and Cochran *et al.* (2006) image the state of the fault zone itself and the surrounding medium before and after the 2004 earthquake, and Shcherbakov *et al.* (2006) examine how the fault region responds temporally with background seismicity and aftershocks. The Li *et al.* (2006) Parkfield study, in conjunction with similar analyses of earthquake effects on other faults (e.g., Li *et al.*, 1998, 2003) provides tantalizing clues about how fault zones are damaged then gradually recover after each large earthquake.

Fault Geometry and Long-Term Behavior of the San Andreas Fault near Parkfield

Bakun *et al.* (2005), Langbein *et al.* (2005), and Thurber *et al.* (2006) reveal an updated 3D view of the San Andreas fault zone in the Parkfield region. They used seismic data from the dense network of Parkfield seismometers, included the 1966 aftershock data of Eaton *et al.* (1970), and applied new methods for relocating earthquakes. The updated picture shows that 1966 aftershocks, background seismicity, and 2004 aftershocks are superimposed (Thurber *et al.*, 2006), indicating that certain locations on the fault fail repeatedly in small earthquakes. This view of the San Andreas is in agreement with that by Waldhauser *et al.* (2004) who imaged the 1969–2002 background seismicity and Eberhart-Phillips and Michael (1993) who imaged the 1966 aftershocks and the background seismicity. The observation of stable microseismicity patterns may disagree with stress change models that predict small earthquake locations purely on the basis of stress changes due to neighboring previous earthquakes (e.g., see Harris [1998], Stein [1999], and Steacy *et al.* [2005] for overview discussions of stress-change calculations). This point, touched upon briefly by Thurber *et al.* (2006), is a topic for continued study.

One use of the newly relocated microseismicity presented by Thurber *et al.* (2006) is to study fault zone structure and evolution. Simpson *et al.* (2006) performed such an analysis and imaged the San Andreas fault zone as a single fault zone at greater than 6-km depth that then transitions to two faults above 6-km depth, the San Andreas fault, and the Southwest Fracture Zone (see Simpson *et al.*, 2006). The Simpson *et al.* (2006) image of the single fault plane at depths greater than 6 km agrees with the earlier study of Eberhart-Phillips and Michael (1993). Murray and Langbein (2006) used the Simpson *et al.* (2006) complex fault geometry in their geodetic modeling of coseismic and postseismic fault slip. This enabled Murray and Langbein (2006) to image the temporal and spatial evolution of the fault slip on the different near-surface strands.

Simpson *et al.* (2006) used the distribution of relocated aftershocks to suggest that the Cholame Valley step-over does not persist to depths greater than 6 km. This step-over has been invoked in previous attempts to explain what does or does not stop Parkfield earthquakes (Lindh and Boore, 1981; Harris and Day, 1999). Instead of a classic pull-apart, Simpson *et al.* (2006) argue that in the near surface in the Parkfield region the San Andreas fault surface is being warped to the northeast over geologic time. This deformation is the result of anelastic (plastic) deformation at shallow depths as the locked section of the fault to the southeast of Parkfield and the creeping section of the fault to the northwest of Parkfield interact, deforming the fault surface in the process. The Simpson *et al.* (2006) model foresees the Southwest Fracture Zone as an increasingly prominent player in San Andreas earthquakes as the principal fault surface readjusts into a simpler, straighter geometry. This pattern of activation and deactivation of adjacent fault surfaces along the San Andreas fault zone at Parkfield is also manifest at long timescales as shown in geologic mapping of Middle Mountain and vicinity (e.g., Sims, 1990; Rymer *et al.*, 2003; Thayer *et al.*, 2004; Thayer, 2006). These studies show that a major fault generally along strike with the Southwest Fracture Zone has accommodated significant long-term slip (in order to juxtapose granites and volcanic rocks of the Pinnacles–Neenach tie [Sims, 1990; Thayer, 2006]), and that there are numerous San Andreas fault-parallel fault surfaces within a couple kilometers of the active San Andreas fault trace that have been active since the Pliocene.

Conclusions

The Parkfield Earthquake Prediction Experiment culminated with a wealth of geophysical and geological data capturing the preseismic, coseismic, and postseismic periods of the 2004 **M** 6.0 Parkfield earthquake. Combined with observations of previous Parkfield earthquakes, the data and models reveal a complex detailed picture of earthquake and fault behavior. The general earthquake and faulting picture at Parkfield can be understood in a broad sense using the scientific tools at hand, but predicting the exact nature of future earthquakes and their resulting ground motions remains a challenge.

Acknowledgments

Many thanks to the Parkfield Chief Scientists, Bill Bakun, Allan Lindh, Evelyn Roeloffs, and John Langbein, and to the more than 100 dedicated technicians and scientists who worked in the field and office on the Parkfield project. Without their tireless efforts over two decades, the 2004 **M** 6.0 event would have been just another California earthquake. We appreciate the hard work of the authors of the special issue, and the enthusiastic, consistent, and thoughtful assistance of BSSA Managing Editor Carol Mark and BSSA Editor-in-Chief Andy Michael. Nathan Toké and John Langbein kindly provided major assistance with the figures, and Norm Abrahamson, Jack Boatwright, and Bob Simpson provided valuable comments on sections of the article. John Langbein and Malcolm Johnston reviewed the entire article and provided many helpful suggestions. This special issue is dedicated to the people who devoted significant parts of their careers to the Parkfield Earthquake Prediction Experiment, but did not live to see the next Parkfield earthquake, including Tom McEvilly, Jerry Eaton, and Sandy Schulz Burford.

References

Allen, C. R., and S. W. Smith (1966). Parkfield earthquakes of June 27–29, 1966, Monterey and San Luis Obispo counties, California—preliminary report, pre-earthquake and post-earthquake surficial displacements, *Bull. Seism. Soc. Am.* **56,** 966–967.

Andrews, D. J., and R. A. Harris (2005). The wrinkle-like slip pulse is not important in earthquake dynamics, *Geophys. Res. Lett.* **32,** L23303, doi 10.1029/2005GL023996.

Andrews, D. J., and R. A. Harris (2006). Reply to comment by Y. Ben-Zion on "The wrinkle-like slip pulse is not important in earthquake dynamics," *Geophys. Res. Lett.* **33,** L06311, doi 10.1029/2006GL025743.

Arrowsmith, R., K. McNally, and J. Davis (1997). Potential for earthquake rupture and M 7 earthquakes along the Parkfield, Cholame, and Carrizo segments of the San Andreas fault, *Seism. Res. Lett.* **68,** 902–916.

Bakun, W. H., and A. G. Lindh (1985). The Parkfield, California, earthquake prediction experiment, *Science* **229,** 619–624.

Bakun, W. H., and T. V. McEvilly (1984). Recurrence models and Parkfield, California earthquakes, *J. Geophys. Res.* **89,** 3051–3058.

Bakun, W. H., B. Aagaard, B. Dost, W. L. Ellsworth, J. L. Hardebeck, R. A. Harris, C. Ji, M. J. S. Johnston, J. Langbein, J. J. Lienkaemper, A. J. Michael, J. R. Murray, R. M. Nadeau, P. A. Reasenberg, M. S. Reichle, E. A. Roeloffs, A. Shakal, R. W. Simpson, and F. Waldhauser (2005). Implications for prediction and hazard assessment from the 2004 Parkfield earthquake, *Nature* **437,** 969–974, doi 10.1038/nature04067.

Ben-Zion, Y. (2006). Comment on "Material contrast does not predict earthquake rupture propagation direction," by R. A. Harris and S. M. Day, *Geophys. Res. Lett.* **33,** L13310, doi: 10.1029/2005GL025652

Ben-Zion, Y., J. R. Rice, and R. Dmowska (1993). Interaction of the San Andreas fault creeping segment with adjacent great rupture zones, and earthquake recurrence at Parkfield, *J. Geophys. Res.* **98,** 2135–2144.

Bilham, R. (2005). Coseismic strain and the transition to surface afterslip recorded by creepmeters near the 2004 Parkfield epicenter, *Seism. Res. Lett.* **76,** 49–57.

Borcherdt, R. D., M. J. S. Johnston, G. Glassmoyer, and C. Dietel (2006). Recordings of the Parkfield 2004 earthquake on the GEOS array: implications for earthquake precursors, fault rupture, and coseismic strain changes, *Bull. Seism. Soc. Am.* **96,** no. 4B, S73–S89.

Brown, R. D., Jr., J. G. Vedder, R. E. Wallace, E. F. Roth, R. F. Yerkes, R. O. Castle, A. O. Waananer, R. W. Page, and J. P. Eaton (1967). The Parkfield-Cholame, California earthquakes of June–August 1966—Surface geologic effects, water-resources aspects, and preliminary seismic data, *U.S. Geol. Surv. Prof. Paper 579*, 66 pp.

Bufe, C. G., P. W. Harsh, and R. O. Burford (1977). Steady-state seismic slip—A precise recurrence model, *Geophys. Res. Lett.* **4,** 91–94.

Cochran, E. S., Y.-G. Li, and J. E. Vidale (2006). Anisotropy in the shallow crust observed around the San Andreas fault before and after the 2004 **M** 6.0 Parkfield earthquake, *Bull. Seism. Soc. Am.* **96,** no. 4B, S364–S375.

Custódio, S., P. Liu, and R. J. Archuleta (2005). The 2004 M_w 6.0 Parkfield, California, earthquake: inversion of near-source ground motion using multiple data sets, *Geophys. Res. Lett.* **32,** L23312, doi 10.1029/2005GL024417.

Dost, B., and H. W. Haak (2006). Comparing waveforms by digitization and simulation of waveforms for four Parkfield earthquakes observed in station DBN, the Netherlands, *Bull. Seism. Soc. Am.* **96,** no. 4B, S50–S55.

Eaton, J. P., M. E. O'Neill, and J. N. Murdock (1970). Aftershocks of the 1966 Parkfield–Cholame, California earthquake: a detailed study, *Bull. Seism. Soc. Am.* **60,** 1151–1197.

Eberhart-Phillips, D., and A. J. Michael (1993). Three-dimensional velocity structure, seismicity, and fault structure in the Parkfield region, central California, *J. Geophys. Res.* **98,** 15,737–15,758.

Fletcher, J. B., P. Spudich, and L. M. Baker (2006). Rupture propagation of the 2004 Parkfield, California, earthquake from observations at the UPSAR array, *Bull. Seism. Soc. Am.* **96,** no. 4B, S129–S142.

Goel, R. K., and C. B. Chadwell (2004). Preliminary report on September 28, 2004 Parkfield earthquake, Earthquake Engineering Research Institute, Oakland, California, www.eeri.org/lfe/pdf/usa_parkfield_goel.pdf. (last accessed June 2006).

Grant, L. B., and K. Sieh (1993). Stratigraphic evidence for seven meters of dextral slip on the San Andreas fault during the 1857 earthquake in the Carrizo Plain, *Bull. Seism. Soc. Am.* **83,** 619–635.

Grant, L. B., and K. Sieh (1994). Paleoseismic evidence of clustered earthquakes on the San Andreas fault in the Carrizo Plain, California, *J. Geophys. Res.* **99,** 6819–6841.

Hardebeck, J. L., J. Boatwright, D. Dreger, R. Goel, V. Graizer, K. Hudnut, C. Ji, L. Jones, J. Langbein, J. Lin, E. Roeloffs, R. Simpson, K. Stark, R. Stein, and J. C. Tinsley (2004) Preliminary report on the 22 December 2003 M 6.5 San Simeon, California, Earthquake, *Seism. Res. Lett.* **75,** 155–172.

Harris, R. A. (1998). Stress triggers, stress shadows, and implications for seismic hazard, introduction to the special issue, *J. Geophys. Res.* **103,** 24,347–24,358.

Harris, R. A. (2004). Numerical simulations of large earthquakes: dynamic rupture propagation on heterogeneous faults, *Pure Appl Geophys.* **161,** no. 11/12, 2171–2181, doi 10.1007/s00024-004-2556-8.

Harris, R. A., and R. J. Archuleta (1988). Slip budget and potential for a M7 earthquake in central California, *Geophys. Res. Lett.* **15,** 1215–1218.

Harris, R. A., and S. M. Day (1997). Effects of a low-velocity zone on a dynamic rupture, *Bull. Seism. Soc. Am.* **87,** 1267–1280.

Harris, R. A., and S. M. Day (1999). Dynamic 3D simulations of earthquakes on en echelon faults, *Geophys. Res. Lett.* **26,** 2089–2092.

Harris, R. A., and S. M. Day (2005). Material contrast does not predict earthquake rupture propagation direction, *Geophys. Res. Lett.* **32,** L23301, doi 10.1029/2005GL023941.

Harris, R. A., and S. M. Day (2006). Reply to "Comment on 'Material contrast does not predict earthquake rupture propagation direction,' by Y. Ben-Zion," *Geophys. Res. Lett.* **33,** L13311, doi 10.1029/2006GL026811.

Harris, R. A., and P. Segall (1987). Detection of a locked zone at depth on the Parkfield, California segment of the San Andreas fault, *J. Geophys. Res.* **92,** 7945–7962.

Hickman, S., M. Zoback, and W. Ellsworth (2004). Introduction to special section: preparing for the San Andreas fault observatory at depth, *Geophys. Res. Lett.* **31,** L12S01, doi 10.1029/20046L020688.

Jackson, D. D., and Y. Y. Kagan (2006). The 2004 Parkfield earthquake, the 1985 prediction, and characteristic earthquakes: lessons for the future, *Bull. Seism. Soc. Am.* **96,** no. 4B, S397–S409.

Jennings, C. W. (1977). Geologic map of California, California Division of Mines and Geology, Geologic Data Map No. 2, scale 1:750,000.

Johanson, I. A., E. J. Fielding, F. Rolandone, and R. Bürgmann (2006). Coseismic and postseismic slip of the 2004 Parkfield earthquake from space-geodetic data, *Bull. Seism. Soc. Am.* **96,** no. 4B, S269–S282.

Johnson, K. M., R. Bürgmann, and K. Larson (2006). Frictional properties on the San Andreas fault near Parkfield, California inferred from models of afterslip following the 2004 earthquake, *Bull. Seism. Soc. Am.* **96,** no. 4B, S321–S338.

Johnston, M. J. S., R. D. Borcherdt, A. T. Linde, and M. T. Gladwin (2006a). Continuous borehole strain and pore pressure in the near-field of the 28 September 2004, **M** 6.0 Parkfield, California, earthquake: implications for nucleation, fault response, earthquake prediction, and tremor, *Bull. Seism. Soc. Am.* **96,** no. 4B, S56–S72.

Johnston, M. J. S., Y. Sasai, G. D. Egbert, and R. J. Mueller (2006b). Seismomagnetic effects from the long-awaited 28 September 2004, **M** 6.0 Parkfield earthquake, *Bull. Seism. Soc. Am.* **96,** no. 4B, S206–S220.

Langbein, J., R. Borcherdt, D. Dreger, J. Fletcher, J. L. Hardebeck, M. Hellweg, C. Ji, M. Johnston, J. R. Murray, and R. Nadeau (2005).

Preliminary report on the 28 September 2004, M 6.0 Parkfield, California earthquake, *Seism. Res. Lett.* **76,** 10–26.

Langbein, J., J. R. Murray, and H. A. Snyder (2006). Coseismic and initial postseismic deformation from the 2004 Parkfield, California, earthquake, observed by Global Positioning System, Electronic Distance Meter, creepmeters, and borehole strainmeters, *Bull. Seism. Soc. Am.* **96,** no. 4B, S304–S320.

Lees, J. M., and C. Nicholson (1993). Three-dimensional tomography of the 1992 Southern California earthquake sequence: constraints on dynamic earthquake rupture? *Geology* **21,** 387–390.

Li, Y.-G., P. Chen, E. S. Cochran, J. E. Vidale, and T. Burdette (2006). Seismic evidence for rock damage and healing on the San Andreas fault associated with 2004 **M** 6.0 Parkfield earthquake, *Bull. Seism. Soc. Am.* **96,** no. 4B, S349–S363.

Li, Y. G., J. E. Vidale, K. Aki, F. Xu, and T. Burdette (1998). Evidence of shallow fault zone strengthening after the 1992 *M* 7.5 Landers, California, earthquake, *Science* **279,** 217–219.

Li, Y. G., J. E. Vidale, S. M. Day, D. D. Oglesby, and E. Cochran (2003). Post-seismic fault healing on the 1999 *M* 7.1 Hector Mine, California earthquake, *Bull. Seism. Soc. Am.* **93,** 854–869.

Lienkaemper, J. J. (2001). 1857 Slip on the San Andreas fault southeast of Cholame, California, *Bull. Seism. Soc. Am.* **91,** 1659–1672.

Lienkaemper, J. J., B. Baker, and F. S. McFarland (2006). Surface slip associated with the 2004 Parkfield, California, earthquake measured on alinement arrays, *Bull. Seism. Soc. Am.* **96,** no. 4B, S239–S249.

Lindh, A. G., and D. M. Boore (1981). Control of rupture by fault geometry during the 1966 Parkfield earthquake, *Bull. Seism. Soc. Am.* **71,** 95–116.

Liu, P., S. Custodio, and R. J. Archuleta (2006). Kinematic inversion of the 2004 **M** 6.0 Parkfield earthquake including an approximation to site effects, *Bull. Seism. Soc. Am.* **96,** no. 4B, S143–S158.

Mena, B., E. Durukal, and M. Erdik (2006). Effectiveness of hybrid Green's function method in the simulation of near field strong motion: an application to the 2004 Parkfield earthquake, *Bull. Seism. Soc. Am.* **96,** no. 4B, S183–S205.

Michael, A. J., and D. Eberhart-Phillips (1991). Relations among fault behavior, subsurface geology, and three-dimensional velocity models, *Science* **253,** 651–654.

Michael, A. J., and L. M. Jones (1998). Seismicity alert probabilities at Parkfield, California, revisited, *Bull. Seism. Soc. Am.* **88,** 117–130.

Murray, J., and J. Langbein (2006). Slip on the San Andreas fault at Parkfield, California, over two earthquake cycles and the implications for seismic hazard, *Bull. Seism. Soc. Am.* **96,** no. 4B, S283–S303.

Murray, J., and P. Segall (2002). Testing time-predictable earthquake recurrence by direct measurement of strain accumulation and release, *Nature* **419,** 287–291, doi 10.1038/nature00984.

Murray, J. R., and P. Segall (2005). Spatiotemporal evolution of a transient slip event on the San Andreas fault near Parkfield, California, *J. Geophys. Res.* **110,** B09407, doi 10.1029/2005JB003651.

Murray, J. R., P. Segall, P. Cervelli, W. Prescott, and J. Svarc (2001). Inversion of GPS data for spatially variable slip-rate on the San Andreas fault near Parkfield, California, *Geophys. Res. Lett.* **28,** 359–362.

Roeloffs, E. (2000). The Parkfield, California earthquake experiment: an update in 2000, *Current Sci.* **79,** no. 9, 1226–1236.

Roeloffs, E., and J. Langbein (1994). The earthquake prediction experiment at Parkfield, California, *Rev. Geophys.* **32,** 315–336.

Rymer, M. J., R. D. Catchings, and M. R. Goldman (2003). Structure of the San Andreas fault zone as revealed by surface geologic mapping and high-resolution seismic profiling near Parkfield, California, *Geophys. Res. Abs.* **5,** 13,523.

Rymer, M. J., J. C. Tinsley, J. A. Treiman, J R. Arrowsmith, K. B. Clahan, A. M. Rosinski, W. A. Bryant, H. A. Snyder, G. S. Fuis, N. Toké, and G. W. Bawden (2006). Surface fault slip associated with the 2004 Parkfield, California, earthquake, *Bull. Seism. Soc. Am.* **96,** no. 4B, S11–S27.

Schorlemmer, D., and S. Wiemer (2005). Microseismicity data forecast rupture area, *Nature* **434,** 1086.

Segall, P., and R. A. Harris (1986). Slip deficit on the Parkfield, California section of the San Andreas fault as revealed by the inversion of geodetic data, *Science* **233,** 1409–1413.

Segall, P., and R. Harris (1987). Earthquake deformation cycle on the San Andreas fault near Parkfield, California, *J. Geophys. Res.* **92,** 10,511–10,525.

Shakal, A., V. Graizer, M. Huang, R. Borcherdt, H. Haddadi, K. Lin, C. Stephens, and P. Roffers (2005). Preliminary analysis of strong-motion recordings from the 28 September 2004 Parkfield, California earthquake, *Seism. Res. Lett.* **76,** 27–39.

Shakal, A., H. Haddadi, V. Graizer, K. Lin, and M. Huang (2006a). Some key features of the strong-motion data from the **M** 6.0 Parkfield, California, earthquake of 28 September 2004, *Bull. Seism. Soc. Am.* **96,** no. 4B, S90–S118.

Shakal, A. F., H. R. Haddadi, and M. J. Huang (2006b). Note on the very high-acceleration Fault Zone 16 record from the 2004 Parkfield earthquake, *Bull. Seism. Soc. Am.* **96,** no. 4B, S119–S142.

Shcherbakov, R., D. L. Turcotte, and J. B. Rundle (2006). Scaling properties of the Parkfield aftershock sequence, *Bull. Seism. Soc. Am.* **96,** no. 4B, S376–S384.

Shimazaki, K., and T. Nakata (1980). Time-predictable recurrence model for large earthquakes, *Geophys. Res. Lett.* **7,** 279–282.

Sieh, K. E. (1978a). Slip along the San Andreas fault associated with the great 1857 earthquake, *Bull. Seism. Soc. Am.* **68,** 1421–1448.

Sieh, K. E. (1978b). Central California foreshocks of the great 1857 earthquake, *Bull. Seism. Soc. Am.* **68,** 1731–1749.

Simpson, R. W, M. Barall, J. Langbein, J. R. Murray, and M. J. Rymer (2006). San Andreas fault geometry in the Parkfield, California, region, *Bull. Seism. Soc. Am.* **96,** no. 4B, S28–S37.

Simpson, R. W., S. S. Schulz, L. D. Dietz, and R. O. Burford (1988). The response of creeping parts of the San Andreas fault to earthquakes on nearby faults: two examples, *Pure Appl. Geophys.* **126,** 665–685.

Sims, J. D. (1990). Geologic map of the San Andreas fault in the Parkfield 7.5-minute quadrangle, Monterey and Fresno Counties, California, U.S. Geol. Surv. Misc. Field Stud. Map MF 2115, scale 1:24,000.

Steacy, S., J. Gomberg, and M. Cocco (2005). Introduction to special section: stress transfer, earthquake triggering, and time-dependent seismic hazard, *J. Geophys. Res.* **110,** doi 10.1029/2005JB003692.

Stein, R. S. (1999). The role of stress transfer in earthquake occurrence, *Nature* **402,** 605–609.

Thayer, M. R. (2006). Structural geology of the San Andreas fault zone at Middle Mountain, near Parkfield, central California, *M.S. Thesis,* Arizona State University, Tempe, 140 pp.

Thayer, M. R., J R. Arrowsmith, J. J. Young, A. K. Fayon, and M. J. Rymer (2004). Geologic structure of Middle Mountain within the San Andreas fault zone near Parkfield, California, *EOS Trans. Am. Geophys. Union* **85,** no. 47, 1335.

Thurber, C., H. Zhang, F. Waldhauser, J. Hardebeck, A. Michael, and D. Eberhart-Phillips (2006). Three-dimensional compressional wavespeed model, earthquake relocations, and focal mechanisms for the Parkfield, California, region, *Bull. Seism. Soc. Am.* **96,** no. 4B, S38–S49.

Titus, S. J., C. DeMets, and B. Tikoff (2006). Thirty-five-year creep rates for the creeping segment of the San Andreas fault and the effects of the 2004 Parkfield earthquake: constraints from alignment arrays, continuous Global Positioning System, and creepmeters, *Bull. Seism. Soc. Am.* **96,** no. 4B, S250–S268.

Toda, S., and R. S. Stein (2002). Response of the San Andreas fault to the 1983 Coalinga–Nuñez earthquakes: an application of interaction-based probabilities for parkfield, *J. Geophys. Res.* **107,** doi 10.1029/2001JB000172.

Toké, N. A., and J R. Arrowsmith (2006). Reassessment of a slip budget along the Parkfield segment of the San Andreas fault, *Bull. Seism. Soc. Am.* **96,** no. 4B, S339–S348.

Toké, N. A., J R. Arrowsmith, J. J. Young, and C. J. Crosby (2006). Pa-

leoseismic and postseismic observations of surface slip along the Parkfield segment of the San Andreas fault, *Bull. Seism. Soc. Am.* **96,** no. 4B, S221–S238.

Toppozada, T., and D. Branum (2006). San Andreas **M** ~6 earthquakes within 40 km of the Priest Valley end zone of the 1857 faulting, *Bull. Seism. Soc. Am.* **96,** no. 4B, S385–S396.

Waldhauser, F., W. L. Ellsworth, D. P. Schaff, and A. Cole (2004). Streaks, multiplets, and holes: high-resolution spatio-temporal behavior of Parkfield seismicity, *Geophys. Res. Lett.* **31,** L18608, doi 10.1029/2004GL020649.

Wang, G.-Q., G.-Q. Tang, C. R. Jackson, X.-Y. Zhou, and Q.-L. Lin (2006). Strong ground motions observed at the UPSAR during the 2003 San Simeon (**M** 6.5) and 2004 Parkfield (**M** 6.0), California, earthquakes, *Bull. Seism. Soc. Am.* **96,** no. 4B, S159–S182.

Weldon, R., K. Scharer, T. Fumal, and G. Biasi (2004). Wrightwood and the earthquake cycle: what a long recurrence record tells us about how faults work, *GSA Today* **14,** no. 9, doi 10.1130/1052–5173.

Xia, K., A. J. Rosakis, H. Kanamori, and J. R. Rice (2005). Laboratory earthquake along inhomogeneous faults: directionality and supershear, *Science* **308,** 681–684, doi 10.1126/science.1108193.

Young, J. J., J R. Arrowsmith, L. Colini, L. B. Grant, and B. Gootee (2002). 3D excavation and measurement of recent rupture history along the Cholame segment of the San Andreas fault, *Bull. Seism. Soc. Am.* **92,** 2670–2688.

U.S. Geological Survey
345 Middlefield Road, MS 977
Menlo Park, California 94025
harris@usgs.gov
(R.A.H.)

Department of Geological Sciences
Arizona State University
Tempe, Arizona 85287
ramon.arrowsmith@asu.edu
(J R.A.)

Manuscript received 9 May 2006.